

The Comparative Study of Photocatalytic Self-Cleaning Properties of Synthesized Nanoscale Titania and Zirconia onto Polyacrylonitrile Fibers

Hadi Fallah Moafi, Abdollah Fallah Shojaie, Mohammad Ali Zanjanchi

Department of Chemistry, Faculty of Science, University of Guilan, Rasht, Iran

Received 12 December 2009; accepted 14 March 2010

DOI 10.1002/app.32463

Published online 10 June 2010 in Wiley InterScience (www.interscience.wiley.com).

ABSTRACT: The photocatalytic activity of TiO₂ and ZrO₂-coated polyacrylonitrile (PAN) fibers was compared through the self-cleaning of methylene blue and eosin yellowish. TiO₂ and ZrO₂ nanocrystals were successfully synthesized and deposited onto PAN fibers with photocatalytic self-cleaning activity using the sol-gel process at low temperature. The pristine and treated samples have been characterized by several techniques, such as scanning electron microscopy, transmission electron microscopy, Fourier transform infrared spectroscopy, diffuse reflectance spectroscopy, X-ray diffraction, and thermogravimetric analysis. The TiO₂ nanoparticles with 10–20 nm in size, and ZrO₂ with 20–40 nm have been synthesized to form

dispersed particles on the fiber surface, which shows photocatalytic properties when exposed to UV-Vis light. The photocatalytic activity, tested by measuring the degradation of adsorbed methylene blue and Eosin Y. Photocatalytic activity of TiO₂-coated fibers toward dyes degradation was higher than that of ZrO₂-coated fibers. This preparation technique can be also applied to new fabrics to create self-cleaning and UV irradiation protection properties in them. © 2010 Wiley Periodicals, Inc. *J Appl Polym Sci* 118: 2062–2070, 2010

Key words: coatings; fibers; photochemistry; photocatalysis; self-cleaning

INTRODUCTION

Among various oxide semiconductor photocatalysts, nanocrystalline TiO₂ is widely used in water^{1–3} and air purification,^{3–5} in self-cleaning process,^{6–8} and as bactericide under light irradiation.^{8–14} TiO₂ coated onto surfaces such as fabrics, glass, cement, and plastics had been recently reported.^{3–12} Recently, fabrics modified with TiO₂ have been the subject of several studies focusing on pretreatment fabric process,^{15–19} coating methods^{20,21} and TiO₂ particles synthesis and deposition.^{16–18,22–26}

Owing to its impressive physical and chemical properties, such as efficient photocatalytic activities, facilitated by its particle size to diffuse the excited electrons and holes towards the surface before recombination, high-oxidizing ability, high-stability, non-toxicity, and low-cost, TiO₂ has been regarded as an ideal photocatalyst.^{27,28} Among all preparation techniques for producing TiO₂, the sol-gel method is the most widely used due to its ability to nucleate anatase at relatively low temperatures,^{29,30} which makes

it suitable for application in materials with low thermal resistance, such as plastics and biomaterials.

Self-cleaning treatment technology of fibers by incorporation of titanium dioxide nanoparticles is a new concept that has been introduced in recent years.^{28,31}

TiO₂ self-cleaning coatings are finding increasing applications in buildings, public furniture, and auto industry. The self-cleaning mechanism is mainly based on TiO₂ photocatalysis, where photoinduced electronholes catalyze reaction on the surface.^{32–34} It is anticipated that self-cleaning fibrous materials would have significant potential in the global commercial market. Therefore, this novel concept continues to open up exciting opportunities for further research and development.

In this study, self-cleaning polyacrylonitrile (PAN) fibers have been modified following a nanotechnology approach in which anatase nanocrystals of titanium dioxide and zirconium dioxide are formulated and carefully applied to the fibers via room temperature sol-gel process. PAN is one of the most important fiber-forming polymers and has been widely used because of its high-strength, abrasion resistance, and good insect resistance. The comparison study of the photocatalytic properties of the synthesized titania and zirconia on PAN fibers is investigated too.

Correspondence to: A. F. Shojaie (a.f.shojaie@guilan.ac.ir).
Contract grant sponsor: University of Guilan.

EXPERIMENTAL

Materials

PAN fiber (PANF) was provided by Daqing Polyacrylonitrile Corp., PRC. The PAN used was a copolymer of 90% acrylonitrile, 10% methylacrylate, and had a diameter of about 20 μm .

Methylene blue (MB) and eosin yellowish (Eosin Y) of AR grade obtained from, Merck (Germany) were used for the experiments. Their physical and chemical properties are shown in Table I. Other chemicals were obtained from Merck (Germany) and used as such without further purification. Water used in our experiments was triply distilled.

Synthesis procedure

The typical procedure for synthesis of nano TiO_2 and ZrO_2 onto PAN fibers is as follows:

Titanium (IV) isopropoxide (TIP) was used as a precursor of TiO_2 . TIP (0.01 mol) was added to absolute ethanol (50 mL) under vigorous stirring conditions and then triethylamine (0.005 mol) was added as a stabilizer of the solution and stirred (200 rpm) for 15 min under an inert environment. Another solution was then prepared separately as follows: hydrochloric acid (1 mL) and water (0.5 mL) were added to ethanol (50 mL) and mixed well by a magnetic stirrer for 10 min. This solution was then added dropwise into above mixture consisting of TIP, ethanol, and triethylamine and stirred vigorously at room temperature to carry out hydrolysis. Subsequently, after continuous stirring for 2 h, the yellowish transparent sol was obtained. The formed TiO_2 sol was transparent and quite stable.

Zirconium chloride (ZrCl_4) was used as the precursor for the synthesis of nano ZrO_2 . The sol was prepared as follows: ZrCl_4 (5 g) was added to absolute ethanol (100 mL) under vigorous stirring condi-

tions and then water (5 mL) was added and stirred (200 rpm) vigorously for 2 h. After continuous stirring for 2 h, stable and transparent sol was obtained.


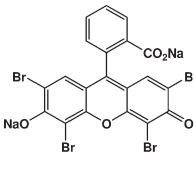
For the impregnation, the fiber samples were treated with acetone for 60 min to remove impurities and dried at room temperature for 24 h. The fibers after dried in a preheated oven are then immersed for 5 min in the TiO_2 and ZrO_2 liquid sol. The extracted samples were then placed in 70°C preheated oven to remove the solvent from the fiber and then heated at 200°C for 15 min, to complete the formation of titanium dioxide and zirconia from the precursor. Finally, the impregnated fibers were treated in distilled water. During this step, the unattached particles were removed from the fiber surface.

Photocatalytic test

The photoactivity of the titanium dioxide and zirconia-coated PAN fibers has been investigated by exposing the samples containing adsorbed MB and Eosin Y to UV-Vis light.

For this purpose, 100 mL aqueous solutions (1.0×10^{-5} M) of MB and Eosin Y were prepared. Both bare and coated fibers are treated in MB and Eosin Y solutions. The same amount of each sample was immersed under mild stirring in the same amount of the solution and remained overnight to complete the adsorption. The solution was then removed and the samples dried at room temperature. The so-obtained samples (coated-fibers) were cut into 2×2 cm^2 , which they have fixed in the front of the integrating sphere hole of the diffuse reflectance attachment. These selected samples were exposed to UV-Vis to test their photoactivity. The similar settings were performed in several intervals during the test. For photocatalytic reactions, the irradiation was carried out on dry samples, by means of a high-pressure mercury lamp (HPMV 400W, Germany). The

TABLE I
Properties of Dyes Used for this Study

Dye	Chemical structure	λ_{max} (nm)	M.W
Methylene blue [3,7-bis(dimethylamino) phenazathionium chloride trihydrate]	 $(\text{C}_{16}\text{H}_{18}\text{ClN}_3\text{S} \cdot 3\text{H}_2\text{O})$	650	373.5 g mol^{-1}
Eosin Y [2,4,5,7-tetra-bromofluorescein di-sodium salt]	 $(\text{C}_{20}\text{H}_6\text{Br}_4\text{Na}_2\text{O}_5)$	515	692 g mol^{-1}

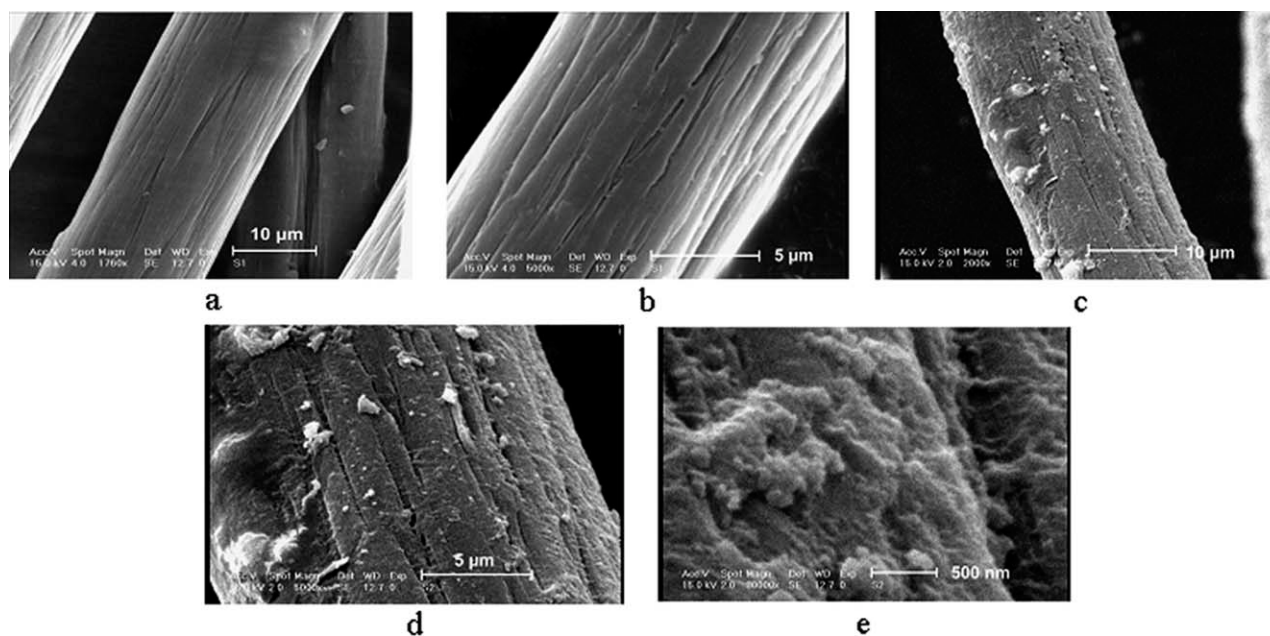


Figure 1 SEM images of: (a) pure fiber (b) enlarged pure fiber, (c) TiO₂-coated fiber, (d–e) enlarged TiO₂-coated fiber.

lamp yields a spectrum ranging from ultraviolet to visible (200–800 nm). The distance between the lamp and reactor was 50 cm, and the intensity of the UV radiation reaching the reactor was measured to be about 20 mW/cm² by a radiometer.

The photocatalytic decomposition rate was determined from the following equation.

$$\text{Photocatalytic decomposition rate} = \frac{C_0 - C}{C_0}$$

where C_0 is the initial concentration of the dyes and C is the final concentration after illumination by UV light. This enabled us to determine the decolorization efficiency (%) according to the equation:

$$\text{Efficiency (\%)} = \frac{C_0 - C}{C_0} \times 100$$

Characterization techniques

To investigate the morphology of the pure and coated fibers, scanning electron microscopy (SEM) images were obtained on a Philips, XL30 equipped with energy dispersive (EDS) microanalysis system for compositional analysis of the TiO₂ and ZrO₂-coated fibers. The TiO₂ and ZrO₂ particle sizes were obtained by transmission electron microscope (TEM) images on a Philips CM10 instrument with an accelerating voltage of 100 kV. For photodecomposition reaction, the UV-Vis reflectance spectra were recorded at room temperature by a UV-2100 Shimadzu Spectrophotometer in the reflectance mode by investigating the evolution of the absorbance. To analyze the PAN polymer chain quality before and after the treatment, FTIR analysis was performed on the samples mixed with KBr. The spectra were recorded with a Vertex70, Bruker spectrometer. X-ray

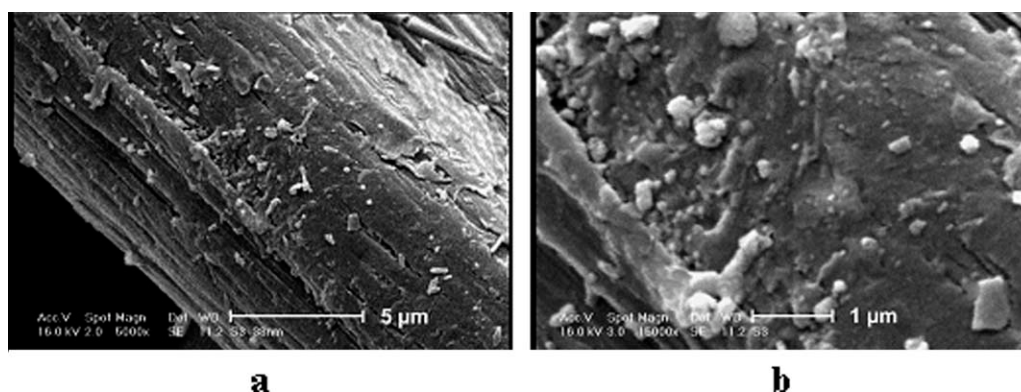


Figure 2 SEM images of: (a) ZrO₂-coated fiber, (b) enlarged ZrO₂-coated fiber.

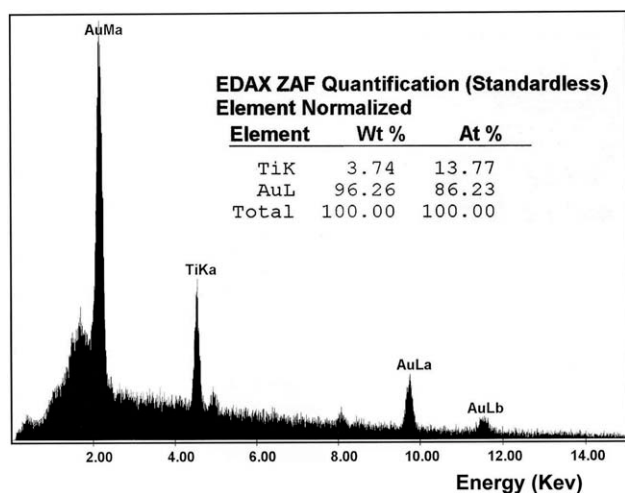


Figure 3 EDS spectra of: TiO_2 -coated polyacrylonitrile fiber after washing.

diffraction (XRD) measurements were recorded by a D8 Bruker Advance diffractometer with $\text{Cu-K}\alpha$ radiation, scan rate $0.02\ 2\theta/\text{s}$ and within a range of 2θ of $10\text{--}70$ at room temperature. To investigate the thermal behavior of samples, thermogravimetric analysis was performed in air flow (ramp of $10^\circ\text{C}/\text{min}$) by thermogravimetric analyzer (TGA V5.1A DuPont 2000).

RESULTS AND DISCUSSION

SEM, TEM images, and EDS analysis

To investigate the morphology of the obtained samples, comparison between the SEM images of the treated and untreated PAN fibers is illustrated in Figures 1 and 2.

Figures 1 and 2 clearly show that treated fibers are covered by a continuous and dispersed TiO_2 and ZrO_2 nanoparticles. SEM study of TiO_2 -coated and

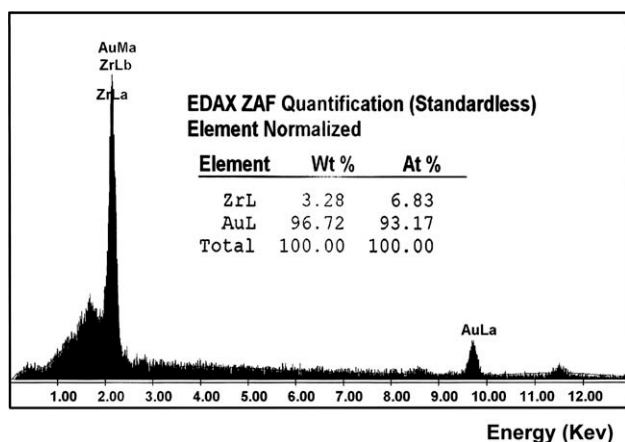
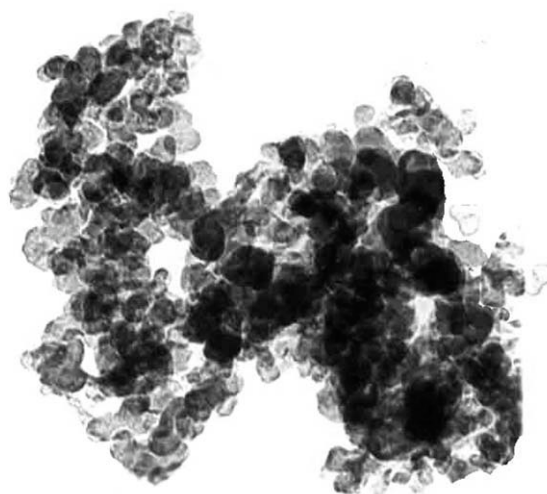


Figure 4 EDS spectra of: ZrO_2 -coated polyacrylonitrile fiber after washing.



50 nm

Figure 5 TEM image of TiO_2 particles forming on the fiber.

ZrO_2 -coated indicate that the particle size of the deposited titania and zirconia on the fibers surface are less than $50\ \text{nm}$ [Figs. 1(e) and 2(b)].

In Figures 3 and 4 the EDS analysis of TiO_2 and ZrO_2 -covered fibers after washing are reported. On the basis of this result, it is noteworthy to observe that the deposited material consists of titanium, zirconium, and oxygen and after washing, remarkable amount of titania and zirconia is still present on the fibers surface. This means that TiO_2 and ZrO_2 particles are firmly anchored to the surface of fibers. The local EDS analysis from the smooth and particles positions showed an average of 1.9 and 7.9 wt % of TiO_2 -coated PAN, respectively. This clearly shows unhomogeneity in titania distribution onto the fiber. The unhomogeneity in the distribution of ZrO_2 on PAN is less, because the average values found for ZrO_2 -coated PAN are 3.3 and 4.9 wt %, respectively.

To investigate the size of TiO_2 and ZrO_2 particles forming on the fibers surface, a portion of the material was collected by scratching the surface and was analyzed by TEM. TEM images, reported in Figures 5 and 6, shows that the deposited titania and zirconia consists of uniform spherical particles of average diameter $10\text{--}20$ and $20\text{--}40\ \text{nm}$ respectively. It is noticeable that the spherical TiO_2 and ZrO_2 particles are distributed homogeneously on the PAN surface.

X-ray diffraction analysis

The XRD patterns of pure and titania-coated PAN are reported in Figure 7. Figure 7(a) shows two peaks: the intense one at 17° and the broad one at 29° , which constitute the typical XRD pattern of

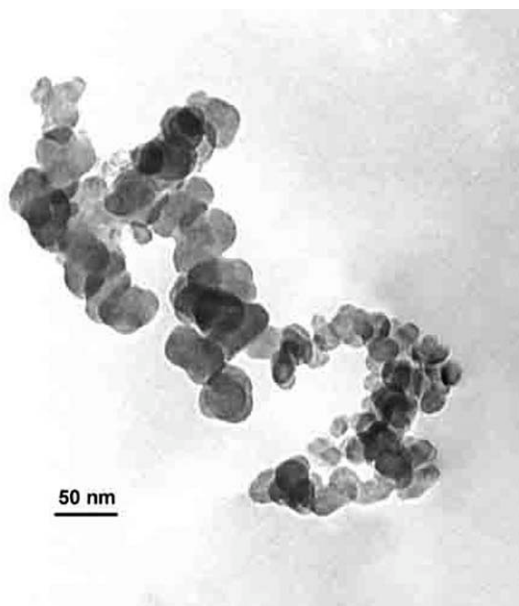


Figure 6 TEM image of ZrO_2 particles forming on the fiber.

PAN fibers.³⁵ Figure 7(b) shows XRD pattern of TiO_2 -covered fibers. As the amount of TiO_2 onto surface fibers was low, therefore TiO_2 on the fibers surface did not show good crystalline phase intensity in XRD pattern. However, small peaks were observed at $2\theta = 25^\circ, 37^\circ$. These are associated with diffraction peaks corresponding to anatase crystallites. Figure 7(c,d) shows XRD patterns of sol-gel derived TiO_2

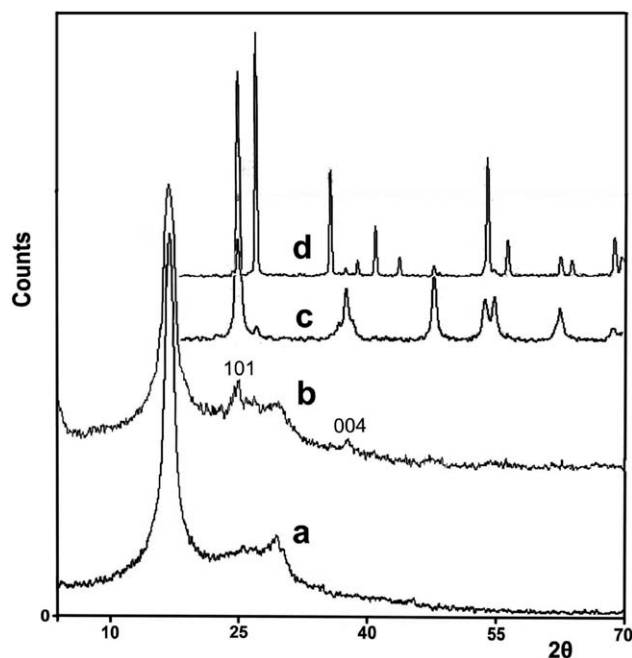


Figure 7 XRD patterns of samples: (a) pure fibers, (b) TiO_2 -covered fibers at $200^\circ C$, (c) sol-gel-derived TiO_2 powder at $200^\circ C$, (d) sol-gel-derived TiO_2 powder at $500^\circ C$, (e) sol-gel-derived TiO_2 powder at $700^\circ C$.

powders from nanosol calcinated at 500 and $700^\circ C$, respectively. TiO_2 powder calcinated at $500^\circ C$ in the spectrum of TiO_2 can be easily identified as the crystal of anatase form, whereas at $700^\circ C$ can be easily taken as the crystal of rutile form.

Figure 8(b) shows XRD pattern of ZrO_2 -covered fibers. Zirconia did not show a crystalline phase. This indicates that the coating of ZrO_2 is predominantly amorphous at low temperature. Figures 8(c–e) shows XRD patterns of sol-gel derived ZrO_2 powders calcinated at $200, 300,$ and $700^\circ C$, respectively. It can be observed that with increasing of temperature zirconia crystalline phase has been manifested [Figs. 8(c,d)]. Figure 8(e) shows the diffraction patterns of the samples treated at $700^\circ C$. The presence of the tetragonal phase was observed to be dominant for zirconium oxide. It was characterized by peaks located at 30.51 and 61.8 (2θ). ZrO_2 mainly contains three polymorphs: monoclinic, tetragonal, and cubic. The monoclinic phase is thermodynamically stable from room temperature to $1200^\circ C$ and transforms to the tetragonal form at 1200 – $2370^\circ C$.

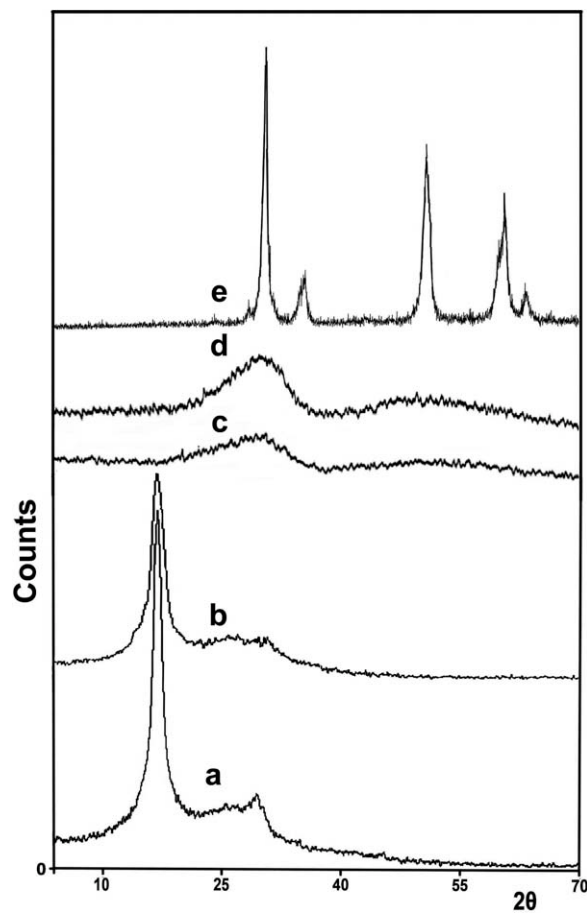


Figure 8 XRD patterns of samples: (a) pure fibers, (b) ZrO_2 -covered fibers at $200^\circ C$, (c) sol-gel-derived ZrO_2 powder at $200^\circ C$, (d) sol-gel-derived ZrO_2 powder at $300^\circ C$, (e) sol-gel-derived ZrO_2 powder at $700^\circ C$.

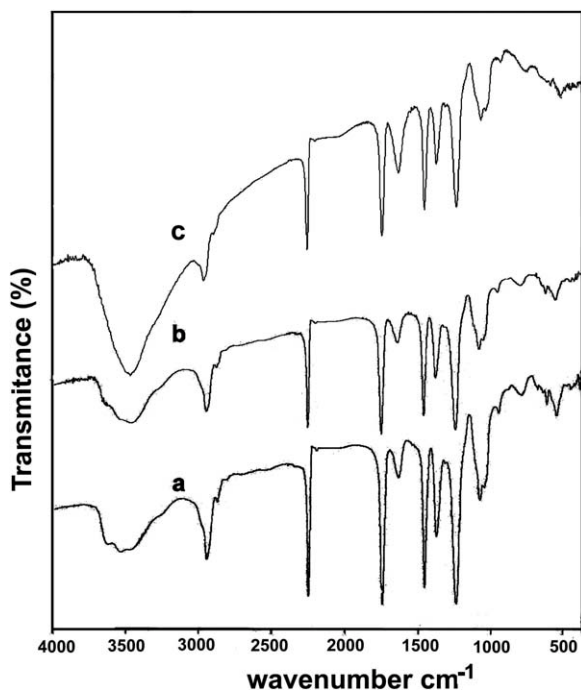


Figure 9 FTIR spectra of: (a) pure polyacrylonitrile fibers, (b) TiO₂-covered fibers, (c) ZrO₂-covered fibers.

The cubic phase appears only at temperatures over 2370°C.³⁶ The synthesis method used enabled us to obtain this phase at a low temperature compared to the much higher temperature (1200°C) reported for this phase in the literature.³⁷

FTIR spectroscopy analysis

In Figure 9, the IR spectra of the PAN fibers before and after treatment are compared (spectrum a–c). It is apparent that peaks of the PAN [Fig. 9(a)] can be assigned as follows: 3630 cm⁻¹ (γ OH), 2941 and 2870 cm⁻¹ (γ C–H asymmetric and symmetric in CH, CH₂, and CH₃ groups), 2244 cm⁻¹ (γ C≡N), 1741 cm⁻¹ (γ C=O), 1455 cm⁻¹ (δ CH₃ and δ_s CH₂), 1374 cm⁻¹ (δ CH₃ symmetric in CCH₃), 1240 cm⁻¹ (γ C–N), 1070 cm⁻¹ (δ C–N), and 535 cm⁻¹ (δ_t C=O), where γ represents a stretching vibration, δ a bending vibration, δ_s a scissor vibration, and δ_t a twisting vibration.³⁸

The spectrum of the fibers after grafting (Fig. 9, spectrum b–c) are substantially unaltered. This means that due to the low external surface area of the supporting fibers, the IR spectroscopy is not informative on the grafting mechanism at all. It is quite remarkable that IR spectrum of the treated sample is totally dominated by the spectrum of the fiber, the contribution of the TiO₂ and ZrO₂ phase (which should appear at $\gamma < 700$ cm⁻¹) is also negligible.

Thermogravimetric analysis

The TGA analysis of the pure and coated-fiber carried out under an air atmosphere at a heating rate of 10°C/min.

The TGA analysis of the PAN fiber in air atmosphere [Fig. 10(A)] can be roughly divided into three steps according to the extent of weight loss.^{39–41} The first step is up to about 250°C, where weight loss is very small. It is inferred that there is only cyclization occurring in this step, as this reaction theoretically does not cause any weight loss.⁴² The second step is up to about 300°C. During this step, the rate of weight loss becomes quite rapid, which is mainly because of the dehydrogenation. It is apparent that the weight loss of PAN/TiO₂ and PAN/ZrO₂ is larger than that of PAN [Figs. 10(B,C)]. It implies that TiO₂ and ZrO₂ have promoted the dehydrogenation to some extent. In the last step, the rate of weight loss is quite steady; but contrarily the weight loss of PAN becomes larger than that of PAN/TiO₂ and PAN/ZrO₂. In this step, fragmentation of polymer chains occurs producing volatile species leading to weight loss.

After combustion of all organic part, the residual amount corresponds to TiO₂ and ZrO₂. From this result, it is evident that the TGA technique in air allows evaluating the existence of TiO₂ and ZrO₂ covering the PAN fibers, as obtained by the synthesis procedure described before.

Photocatalytic degradation

The photoactivity of the synthesized titanium dioxide and zirconium dioxide nanoparticles on PAN fibers has been investigated by exposing the samples

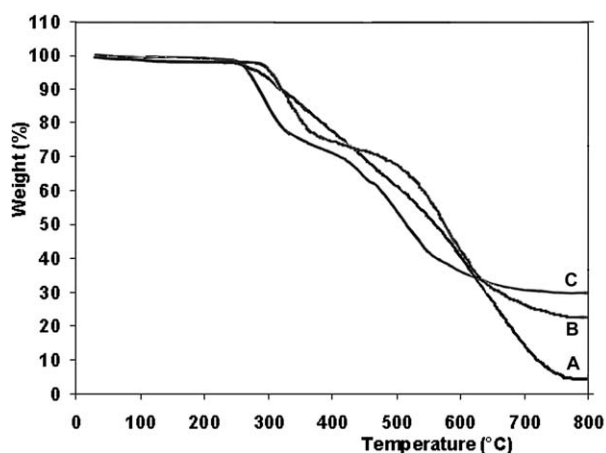


Figure 10 TGA curves in air: (A) polyacrylonitrile fiber, (B) TiO₂-coated fiber and (C) ZrO₂-coated fiber. The residual weight of the sample, recorded at 800°C, is related to the TiO₂ and ZrO₂ content, after that the polyacrylonitrile fiber burning has taken place.

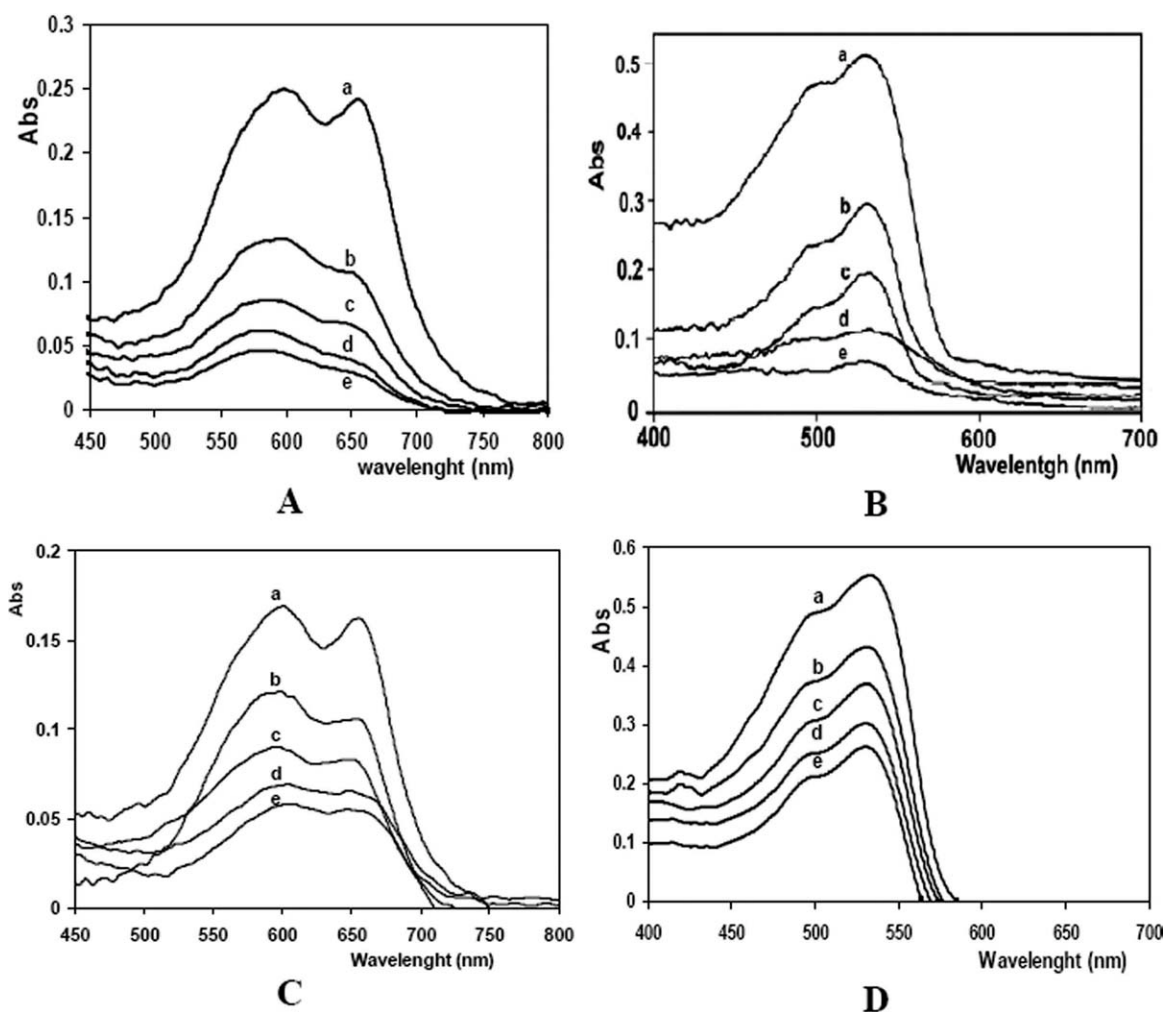


Figure 11 UV-Vis reflectance spectra of dyes on coated fibers. (A) UV-Vis reflectance spectra of methylene blue (MB) on TiO_2 -coated fibers at room temperature, under UV-Vis light irradiation: no exposure (a), irradiation for 2 h (b), 4 h (c), 6 h (d), and 8 h (e). (B) Eosin Y on TiO_2 -coated fibers, (C) Methylene blue (MB) on ZrO_2 -coated fibers, (D) Eosin Y on ZrO_2 -coated fibers.

containing adsorbed MB and Eosin Y to UV-Vis light. Changes of dyes absorption band in the during photocatalysis process with titania and zirconia-coated and pristine fibers are investigated. The photodecomposition was conducted for 8 h at a temperature of 303 K.

The UV-Vis reflectance spectra obtained on the dried samples before (spectrum a) and after illumination (spectrum b–e) are presented in Figure 11. From Figures 11(A,B), it can be observed that the absorption bands in the 500–700 nm and 450–600 nm intervals because of adsorption of MB and Eosin Y change rapidly because supported TiO_2 promotes the catalytic photodegradation [spectrum b–e in Figures 11(A,B)]. This is not unexpected as the photocatalytic activity of TiO_2 is well known.^{43,44} The photocatalytic degradation rate of the absorption bands of dyes adsorbed on the TiO_2 -covered fibers is much higher than that observed in case of untreated fibers (Fig. 12). Of course the photodegradation effect is lower than that observed on P25

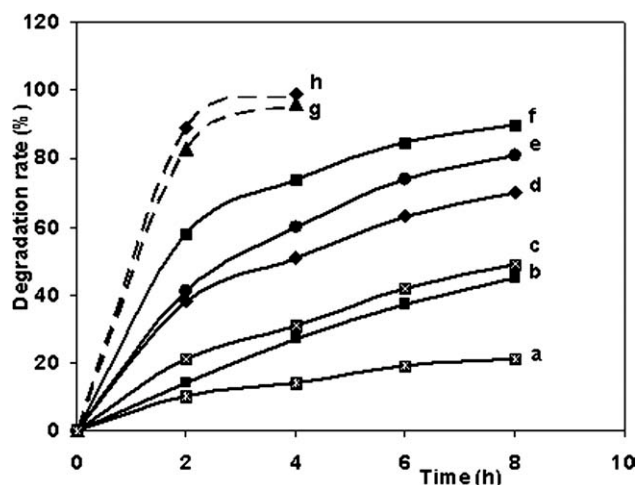


Figure 12 Photocatalytic decomposition rate of methylene blue and Eosin Y vs. irradiation time. (a) MB on untreated fibers, (b) Eosin Y on untreated fibers, (c) Eosin Y on ZrO_2 -coated fibers, (d) MB on ZrO_2 -coated fibers, (e) Eosin Y on TiO_2 -coated fibers, (f) MB on TiO_2 -coated fibers, (g) Eosin Y on P25 (Degussa), (h) MB on P25 (Degussa).

(Degussa), which is the best TiO₂ catalyst. However, the photocatalytic activity of titania is dependent on both particle size and degree of crystallization.⁴⁵

Similar results have been obtained for the photocatalytic activity ZrO₂-covered fibers to photodegradation of adsorbed MB and Eosin Y [Figs. 11(C,D)]. The photocatalytic degradation rate of dyes adsorbed on the ZrO₂-covered fibers is higher than that observed in case of untreated fibers (Fig. 12). However, photocatalytic activity of TiO₂-coated fibers toward dyes degradation was much better than that of ZrO₂-coated fibers [Figs. 12(e,f)]. It can be observed that the highest effectiveness of dye degradation on TiO₂-coated fibers was obtained. After 8 h of the process performance, change of the dye concentration in the surface of fiber, in case of ZrO₂-coated fibers is lower than that observed on TiO₂-coated fibers. On the other hand, the lowest degradation efficiency was found in case ZrO₂-coated fiber.

The main reason for this greater activity of TiO₂ is that band-gap energy (E_g) for titania (3.2 eV) is lower than that in case of zirconia (4.5 eV).⁴⁶ The charge separation within semiconductor particles and subsequent electron transfer to O₂ for producing active oxygen radicals (e.g., O₂•⁻, •OOH, •OH)⁴⁷⁻⁴⁹ are important to the efficiency of the dye photodegradation under both UV and visible light irradiation. Therefore, the charge separation and subsequent electron transfer in TiO₂ is easily excited with UV-Vis irradiation.

It is evident that TiO₂-covered fibers promote the photodegradation process and the high surface area associated with the small particle size ensures a favorable condition for a relatively fast degradation.

CONCLUSIONS

In this contribution, a comparison of effectiveness of dyes decomposition on PAN, using TiO₂ and ZrO₂ as a semiconductor photocatalyst is presented. Nanosized titania and zirconia were successfully prepared by sol-gel technique at low temperature on PAN fiber to study performance of photocatalytic self-cleaning activity. This innovation is important because it should allow its practical use for industrial applications.

Photodecomposition of MB and eosin yellowish as target materials preadsorbed on PAN fibers containing ZrO₂ and TiO₂ was monitored. Comparison of photocatalytic activity of the two semiconducting materials has clearly indicated that TiO₂ is the most active photocatalyst in the degradation of MB and eosin Y using UV-Vis light as a energy source. Photodegradation rate of dyes using TiO₂ onto surface fibers was much better than that using ZrO₂.

Supported TiO₂ particles on PAN textiles promote the photodegradation process and the high-surface area associated with the small particle size ensures a favorable condition for self-cleaning purposes.

References

- Torres, R. A.; Nieto, J. I.; Combet, E.; Petrier, C.; Pulgarin, C. *Appl Catal B* 2008, 80, 168.
- Gumy, D.; Giraldo, S. A.; Rengifo, J.; Pulgarin, C. *Appl Catal B* 2008, 78, 19.
- Brosillon, S.; Lhomme, L.; Vallet, C.; Bouzaza, A.; Wolbert, D. *Appl Catal B* 2008, 78, 232.
- Coronado, J. M.; Suarez, S.; Portela, R.; Sanchez, B. *J Adv Oxid Technol* 2008, 11, 362.
- Xiao, G.; Wang, X.; Li, D.; Fu, X. *J Photochem Photobiol A* 2008, 193, 213.
- Yuranova, T.; Sarria, V.; Jardim, W.; Rengifo, J.; Pulgarin, C.; Trabesinger, G.; Kiwi, J. *J Photochem Photobiol A* 2007, 188, 334.
- Tung, W. S.; Daoud, W. A. *Acta Biomater* 2009, 5, 50.
- Kasanen, J.; Suvanto, M.; Pakkanen, T. T. *J Appl Polym Sci* 2009, 111, 2597.
- Sayilkan, F.; Asilturk, M.; Kiraz, N.; Burunkaya, E.; Arpac, E.; Sayilkan, H. *J Hazard Mater* 2009, 162, 1309.
- Caballero, L.; Whitehead, K. A.; Allen, N. S.; Verran, J. *J Photochem Photobiol A* 2009, 202, 92.
- Zhao, J.; Krishna, V.; Hua, B.; Moudgil, B.; Koopman, B. *J Photochem Photobiol A* 2009, 94, 96.
- Chung, C. J.; Chiang, C. C.; Chen, C. H.; Hsiao, C. H.; Lin, H. I.; Hsieh, P. Y.; He, J. L. *Appl Catal B* 2008, 85, 103.
- Nadtochenko, V.; Denisov, N.; Sarkisov, O.; Gumy, D.; Pulgarin, C.; Kiwi, J. *J Photochem Photobiol A* 2006, 181, 401.
- Gumy, D.; Morais, C.; Bowen, P.; Pulgarin, C.; Giraldo, S.; Hajdu, R.; Kiwi, J. *Appl Catal B* 2006, 63, 76.
- Yuranova, T.; Laub, D.; Kiwi, J. *Catal Today* 2007, 122, 109.
- Qi, K.; Xin, J. H.; Daoud, W. A. *Int J Appl Ceram Technol* 2007, 4, 554.
- Bozzi, A.; Yuranova, T.; Kiwi, J. *J Photochem Photobiol A* 2005, 172, 27.
- Bozzi, A.; Yuranova, T.; Guasaquillo, I.; Laub, D.; Kiwi, J. *J Photochem Photobiol A* 2005, 174, 156.
- Meilert, K. T.; Laub, D.; Kiwi, J. *J Mol Catal A Chem* 2005, 237, 101.
- Dong, Y.; Bai, Z.; Liu, R.; Zhu, T. *Atmos Environ* 2007, 41, 3182.
- Ku, Y.; Ma, C. M.; Shen, Y. S. *Appl Catal B* 2001, 34, 181.
- Tung, W. S.; Daoud, W. A. *J Colloid Interface Sci* 2008, 326, 283.
- Uddin, M. J.; Cesano, F.; Scarano, D.; Bonino, F.; Agostini, G.; Spoto, G.; Bordiga, S.; Zecchina, A. *J Photochem Photobiol A* 2008, 199, 64.
- Liuxue, Z.; Xiulian, W.; Peng, L.; Zhixing, S. *Surf Coat Technol* 2007, 201, 7607.
- Uddin, M. J.; Cesano, F.; Bonino, F.; Bordiga, S.; Spoto, G.; Scarano, D.; Zecchina, A. *J Photochem Photobiol A* 2007, 189, 286.
- Yuranova, T.; Mosteo, R.; Bandara, J.; Laub, D.; Kiwi, J. *J Mol Catal A* 2006, 244, 160.
- Fujishima, A.; Honda, K. *Nature* 1972, 238, 37.
- Anpo, M.; Shima, T.; Kodama, S.; Kubokawa, Y. *J Phys Chem* 1987, 91, 4305.
- Daoud, W. A.; Xin, J. H. *J Sol-Gel Sci Technol* 2004, 29, 25.
- Peplow, M. *Nature* 2004, 429, 620.
- Bickmore, C. R.; Waldner, K. F.; Baranwal, R.; Hinklin, T.; Treadwell, D. R.; Laine, R. M. *J Eur Ceram Soc* 1998, 18, 287.

32. Fujishima, A.; Zhang, X.; Tryk, D. A. *Surf Sci Rep* 2008, 63, 515.
33. Fujishima, A.; Rao, T. N.; Tryk, D. A. *J Photochem Photobiol C* 2000, 1, 1.
34. Fujishima, A.; Zhang, X. *C R Chim* 2006, 9, 750.
35. Sanchez-Soto, P. J.; Aviles, M. A.; Del Rio, J. C.; Gines, J. M.; Pascual, J.; Perez-Rodriguez, J. L. *J Anal Appl Pyrol* 2001, 58, 155.
36. Hannink, R. H. J.; Kelly, P. M.; Muddle, B. C. *J Am Ceram Soc* 2000, 83, 461.
37. Wells, A. F. *Structural Inorganic Chemistry*; Oxford University Press: London, 1975.
38. Deng, S.; Bai, R.; Chen, J. P. *J Colloid Interf Sci* 2003, 260, 265.
39. Ouyang, Q.; Cheng, L.; Wang, H.; Kaixi, L. *Polym Degrad Stab* 2008, 93, 1415.
40. Herrera, M.; Wilhelm, M.; Matuschek, G.; Kettrup, A. *J Anal Appl Pyrol* 2001, 58, 173.
41. Grzyb, B.; Machnikowski, J.; Weber, J. V.; Koch, A.; Heintz, O. *J Anal Appl Pyrol* 2003, 67, 77.
42. Bajaj, P.; Sreekumar, T. V.; Sen, K. *Polymer* 2001, 42, 1707.
43. Sandola, F.; Balzani, V. *Photocatalysis—Fundamentals and Applications*, Serpone, N., Pelizzetti, E., Eds.; Wiley: New York, 1989.
44. Kutsuna, S.; Toma, M.; Takeuchi, K.; Ibusuki, T. *Environ Sci Technol* 1999, 33, 1071.
45. Zhang, Z.; Wang, C. C.; Zakaria, R.; Ying, J. Y. *J Phys Chem B* 1998, 102, 10871.
46. Karunakaran, C.; Dhanalakshmi, R. *Sol Energy Mater Sol Cells* 2008, 92, 1315.
47. Zhao, J.; Wu, T.; Oikawa, K.; Wu, K.; Hidaka, H.; Serpone, N. *Environ Sci Technol* 1998, 32, 2394.
48. Wu, T.; Liu, G.; Zhao, J.; Hidaka, H.; Serpone, N. *J Phys Chem B* 1998, 102, 5851.
49. Liu, G.; Wu, T.; Lin, T.; Zhao, J. *Environ Sci Technol* 1999, 33, 1379.